

Fundamental Studies of Soot Deposition Using Flow-through Substrates

Authors: S. Payne ¹; N. Collings ¹; M. V. Twigg ²

¹ Department of Engineering, University of Cambridge, UK.

² Johnson Matthey, Royston, Herts. UK.

Abstract:

Flow-through ceramic substrates were loaded with a commercial soot generator (designed to reproduce the size distribution and composition of particulate emissions from a diesel car engine) in order to investigate deposition on the leading edge and blocking of channels, which is commonly observed on a diesel oxidation catalyst in real-world operation. The pressure drop across the substrates rises linearly with mass of soot collected while channels remain unbridged; the corresponding mass deposition efficiency remained 6.1% for a substrate comprising 1.5×10^4 channels. Long-term loading of this same substrate was carried out until the maximum pressure drop permissible by the soot rig blower was incurred; while by visual inspection 90% of channels were plugged, leading to increasing pressure losses associated with inertial effects, the instantaneous mass deposition efficiency at termination of loading was 17.4%. Optical and electron micrographs of diesel soot deposits were captured to gain insight on the nature of bridging between wall edges and subsequent soot cake build-up; the images exhibit the coral-like structure of soot accumulated around channel entrances.

Concurrently, monodisperse particulates selected by a differential mobility analyser (DMA) from soot generated by a laminar propane flame were delivered to the same substrates in order to investigate deposition by diffusion and the effect of the soot charge state. Results for the unconditioned DMA output (i.e. singly-charged particulates) showed slightly less deposition than predicted by numerical solutions given by Hinds (1999) for diffusional deposition of uncharged spheres from laminar flow. Deposition of NaCl aerosol (comprising single, cubic crystals) of the same electrical mobility diameter was marginally less than for the fractal soot for size cuts at 200 nm and below; this difference diminished as the flow rate increased. At 300 nm, soot deposition changed little over the range of flow rates examined. The soot charge state was then altered from that emerging from the DMA using a bipolar charge conditioner, first alone and then upstream of an electrostatic precipitator. Repeatable reductions in deposition efficiency were observed when the fraction of charged particulates decreased, revealing the action of static charge electric fields on the ceramic surface. The increase in deposition over that by diffusion is plotted as a function of the charged fraction for several particle size cuts and resembles a fractional power law.

Fundamental Studies of Soot Deposition Using Flow-Through Substrates

Simon Payne¹, Nick Collings¹ and Martyn Twigg²

¹ Department of Engineering, University of Cambridge, UK.
² Johnson Matthey, Royston, Hertfordshire, UK.



Introduction

Two concurrent studies of soot collection by cordierite flow-through substrates were conducted in order to investigate the separate mechanisms governing deposition. The substrates each consist of a uniform array of $\sim 10^4$ square channels in which deposition of monodisperse soot was measured at low volume flow rates and compared to a numerical solution for diffusion of particles shown on the right. Substrates were also loaded with a commercial soot generator (designed to reproduce the size distribution and composition of particulate emissions from a diesel car engine) in order to investigate deposition on the upstream end and blocking of channels.

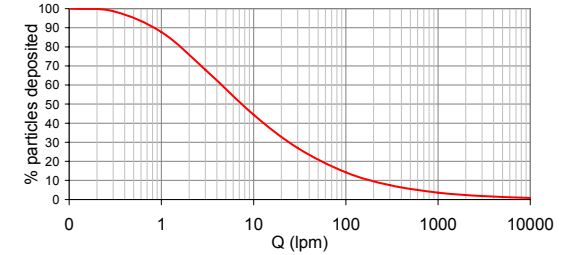
Diffusional deposition of aerosol particles from a fully developed laminar flow to the walls of a single channel is characterised by a dimensionless deposition parameter, defined by Hinds (1) below:

$$\mu = \frac{D_p L}{Q} = \frac{D_p}{d_h^2} \cdot \frac{L}{U} = \frac{\tau_c}{\tau_D} \quad \text{Inverse: } \frac{\tau_D}{\tau_c} = Pe \cdot \frac{d_h}{L}$$

(D_p is the particle diffusivity, L is the channel length, Q is the volume flow rate, d_h is the hydraulic diameter, U is the flow velocity, τ_c and τ_D are the time constants for convection and diffusion, and Pe is the Peclet number for mass transfer.) Penetration is given by the solution below, which is a simplified version of that derived in (2) and is plotted in Fig 1.

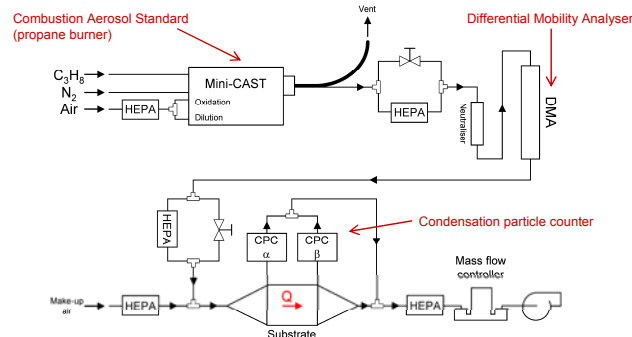
$$\eta_{out}/\eta_{in} = 1 - 5.50 \mu^{2/3} + 3.77 \mu \quad \text{for } \mu < 0.009$$

$$\eta_{out}/\eta_{in} = 0.819 \exp(-11.5 \mu) + 0.0975 \exp(-70.1 \mu) \quad \text{for } \mu \geq 0.009$$

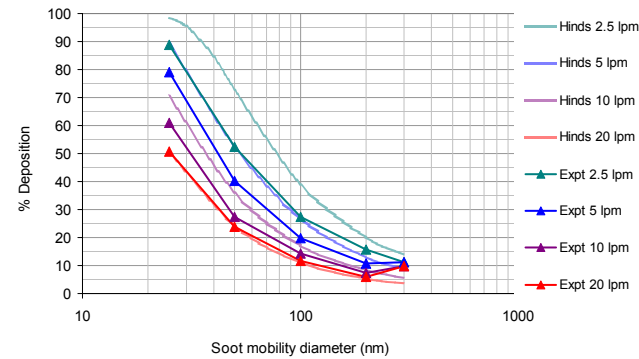


▲ Fig 1: Laminar deposition efficiency of 100nm particles versus volume flow rate calculated for 600 cpsl, ϕ 5.66 in by 6 in flow-through substrate

Size dependence of deposition mechanisms at low volume flow rates

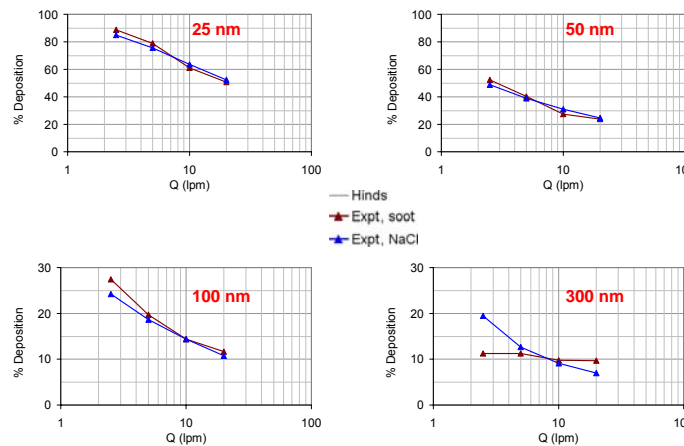


▲ Fig 2: Schematic of set-up examining monodisperse soot deposition efficiency



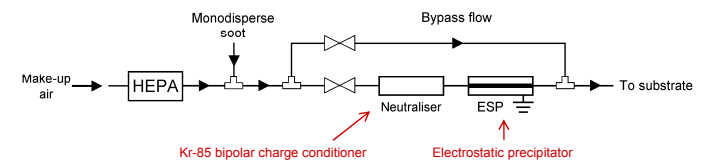
▲ Fig 3: Deposition curves for 600 cpsl, ϕ 4.66 in by 6 in cordierite substrate

Monodisperse soot particulates selected by a differential mobility analyser (DMA) from soot generated by a laminar propane flame were delivered to flow-through substrates as shown in Fig 2 in order to investigate deposition by diffusion and the effect of the soot charge state. Results in Fig 3 for the unconditioned DMA output (i.e. singly charged particulates) showed less deposition than predicted by the numerical solution given above for uncharged spheres. Fig 4 shows that deposition of NaCl aerosol of the same electrical mobility diameter was less than the fractal soot at the lowest flow rates while the difference was insubstantial at higher flow rates; however at 300nm soot deposition changes little over the flow rates examined while the NaCl deposition curve still follows the form expected for diffusion.

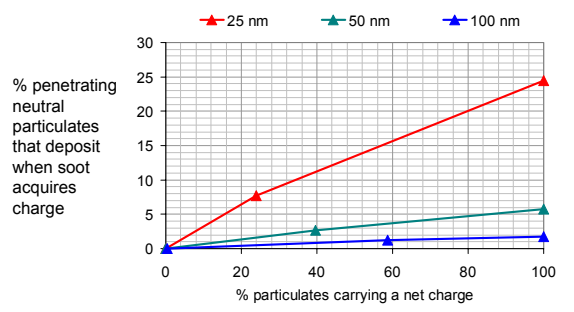


▲ Fig 4: Comparison of deposition efficiency for fractal soot and NaCl particles (single, cubic crystals)

The soot charge state was then altered from that emerging from the DMA using a bipolar charge conditioner, first alone and then upstream of an electrostatic precipitator (see Fig 5). Repeatable reductions in deposition efficiency were observed when the fraction of charged particulates decreased, revealing the action of static charge electric fields on the ceramic surface. The increase in deposition over that by diffusion is plotted as a function of the charged fraction for several particle size cuts in Fig 6 and resembles a fractional power law.

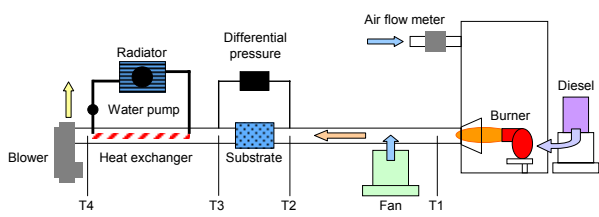


▲ Fig 5: Schematic of set-up for conditioning soot charge state

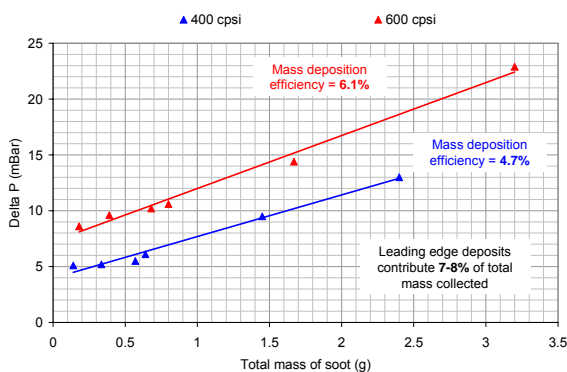


▲ Fig 6: Effect of soot charge state on deposition efficiency

Measurements of diesel PM deposits at standard exhaust flow rates

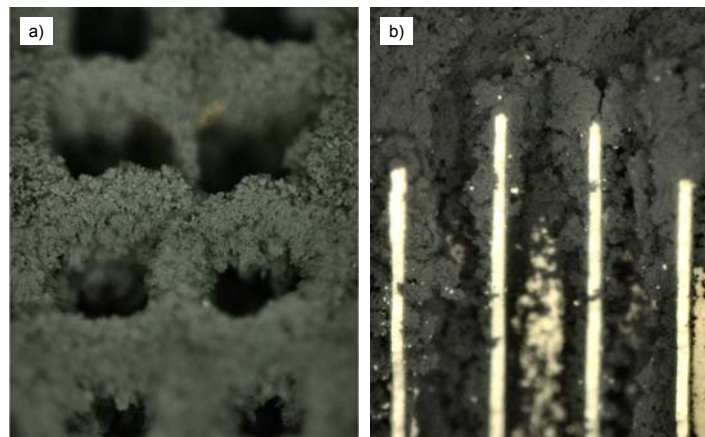


▲ Fig 7: Schematic of Johnson Matthey soot rig

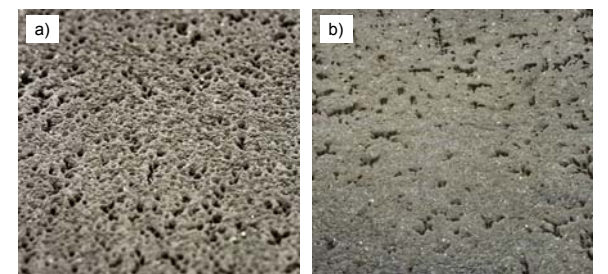


▲ Fig 8: Pressure drop versus total mass of diesel PM collected by 400 and 600 cpsl cordierite substrates (both ϕ 4.66 in by 6 in)

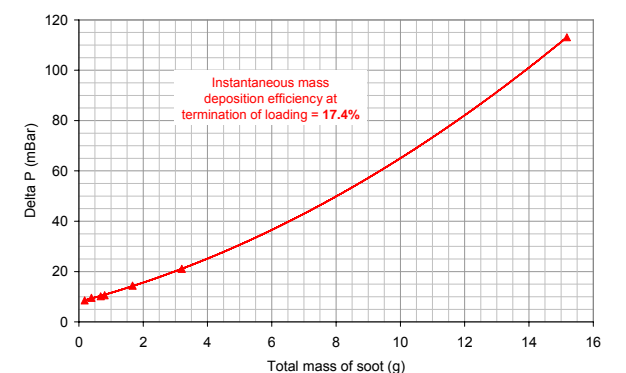
Blocking of substrate channels arising from deposition on the leading edge is commonly observed on a diesel oxidation catalyst (DOC) in real-world operation and inertial impaction on the upstream end was considered the dominant deposition mechanism in a study by Johnson and Kittelson (3). Substrates were loaded with soot generated by a diesel burner (see Fig 7) and the pressure drop rose linearly with mass collected while channels remain unbridged by soot deposits (Fig 8). Detailed optical micrographs presented in Fig 9 exhibit the dendritic morphology of deposits and indicate the profile of deposition beyond channel entrances. Long-term loading of substrates was undertaken to block significant numbers of channels and establish a soot cake, as shown in Fig 10; inertial effects then become significant. While the pressure drop exceeds 100mBar in Fig 11 when $\sim 90\%$ channels are blocked, mass deposition efficiency remains $<20\%$.



▲ Fig 9: Optical micrographs showing diesel PM deposited on a 600 cpsl substrate where a) shows the leading edge and b) shows the channels of a fractured slice (the cell internal width is 0.94 mm)



▲ Fig 10: Photographs of diesel PM deposited on the central region of the leading edge of a 600 cpsl substrate loaded for a) 14 hours and b) 24 hours



▲ Fig 11: Pressure drop versus total soot mass collected by 600 cpsl substrate

Conclusions

- Deposition of soot at low flow rates was slightly less than that predicted by numerical solutions for diffusion of spheres from laminar flow.
- Soot deposition was slightly greater than NaCl deposition at the lowest flow rates for the same size cut, except at 300 nm where soot deposition changes little over the flow rates examined.
- The increase in deposition over that by diffusion due to the electrostatic force resembles a fractional power law when plotted as a function of the soot charged fraction.
- Loading of substrates at standard diesel exhaust flow rates facilitates study of soot bridging behaviour.
- The flow through the substrate remains Darcian while few channels are plugged; pressure losses that scale with U^2 are incurred when significant portions of cake form, yet instantaneous mass deposition efficiency did not exceed 20% when the majority of channels were blocked.

References

1. Hinds, W. C., "Aerosol Technology: Properties, Behavior and Measurement of Airborne Particles", John Wiley and Sons, New York (1999)
2. Bowen, B.D, Levine, S., and Epstein, N., "Fine particle deposition in laminar flow through parallel plate and cylindrical channels", Journal of Colloid and Interface Science 54 (1976) 375-390
3. Johnson, J. E., and Kittelson, D. B., "Deposition, diffusion and adsorption in the diesel oxidation catalyst", Applied Catalysis B: Environmental 10 (1996) 117-137

Acknowledgements

The authors wish to thank the following people for help and advice:

- Jeremy Gidney and Owen Russell at Johnson Matthey Emission Control Technologies
- Martyn Twigg's group at the Johnson Matthey Orchard Laboratories
- Jon Symonds, Kingsley Reavell and Tim Hands at Cambustion

This project is funded by the UK Engineering and Physical Sciences Research Council and Johnson Matthey.